Catalase-peroxidase: KatG

Ignacio Fita[†], *Peter C Loewen*[‡], *and Xavi Carpena*[‡]

[†]Institut de Biologia Molecular de Barcelona (IBMB-CSIC), Barcelona, Spain
[‡]University of Manitoba, Winnipeg, Canada

FUNCTIONAL CLASS

Enzyme; hydrogen peroxide oxidoreductase; catalase-peroxidase or KatG; hydroperoxidase I; EC 1.11.1.21.

Catalase-peroxidases or KatGs are heme-containing enzymes phylogenetically related to the class I family from the superfamily of nonanimal peroxidases, one of the two main heme peroxidase superfamilies.[2–4] Of the two catalytic activities that give rise to the name of catalase-peroxidase, the dominant is the catalase (or catalatic) activity that dismutates hydrogen peroxide to dioxygen and water ($2H_2O_2 \rightarrow O_2 + 2H_2O$). For the much slower peroxidatic reaction, KatGs can employ a broad range of organic electron donors, albeit none yet characterized *in vivo*, to reduce hydrogen peroxide ($H_2O_2 + 2A + 2H^+ \rightarrow 2H_2O + 2A^{\bullet+}$). Despite the predominant catalase activity, KatG does not share any sequence or structural similarity with monofunctional heme catalases. In fact, KatGs are even more catalytically versatile than the name catalase-peroxidase suggests as they can catalyze a variety of other reactions including the cleavage of diimide from isonicotinic acid anhydride (also known as isoniazid or INH, a common antitubercular pro-drug, CAS 0000054-85-3), NADH oxidation, and the formation of isonicotinyl-NAD (the activated form of INH).[5]

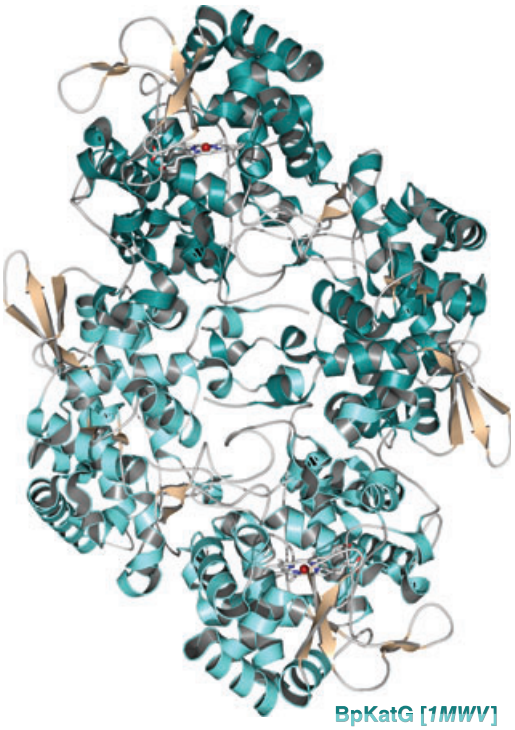

3D Structure Schematic representation of the structure of *Burkholderia pseudomallei* (BpKatG) dimer viewed down the molecular twofold axis (PDB code: 1 MWV). Heme groups are shown as ball-and-sticks for the two subunits (depicted in light and dark teal color). The iron atom is indicated in red. All structural figures were prepared with program PyMOL.[1]

This article was published in the *Encyclopedia of Inorganic and Bioinorganic Chemistry* in 2015 by John Wiley & Sons, Ltd.
DOI: 10.1002/9781119951438.eibc2273

OCCURRENCE

KatGs are found predominantly in eubacteria and archaea, but with two evolutionary branches in lower eukaryotes. KatGs appear to have evolved much later than heme monofunctional catalases, and the presence in archaea and eukaryotes has been attributed to lateral gene transfer.[6] The phylogeny of KatGs was recently reviewed in the context of the evolution of the whole class I family of peroxidases revealing that predecessors of KatGs appear to be at the origin of the nonanimal peroxidase superfamily.[3] The biological importance of the catalase reaction is evident in the observation that most aerobic organisms express multiple catalases and/or KatGs in response to oxidative stress and to the stage of growth.[7] There are, however, some species such as the mycobacteria that express just one KatG as the unique catalase of the organism.[8]

BIOLOGICAL FUNCTION

Hydrogen peroxide is produced as a byproduct of many biological processes and also as a protective response by neutrophils against bacterial infection. Another highly reactive oxidant, superoxide ion, is also generated in many biological processes, and it is converted into H_2O_2 by superoxide dismutase, a key antioxidant enzyme. The combination of H_2O_2 and metal ions produces highly reactive and damaging hydroxyl radicals (such as the Fenton reaction, in case of the iron), and peroxidases and catalases have evolved as efficient antioxidant defenses converting H_2O_2 into H_2O (in peroxidases) or into O_2 and H_2O (in catalases). Thus, the principal role of KatGs appears to be as a protective antioxidant to metabolize H_2O_2 before it is converted into more damaging radical species. This is best illustrated in *Escherichia coli* where the expression of KatG (also known as HPI) is induced by H_2O_2 and other oxidants under the control of the OxyR regulon.[9,10] H_2O_2 can also play important biological roles, particularly as secondary messenger in cell regulation[11–13] and its processing by catalases or peroxidases should be compatible with these roles.

AMINO ACID SEQUENCE INFORMATION

Amino acid sequences

The explosion in genomic sequencing has resulted in the annotation of KatG sequences, commonly corresponding to polypeptides of 700–750 residues, in hundreds if not thousands of different organisms (Figure 1). The first KatG sequence[16] revealed a close relationship to nonanimal heme peroxidases but one that was repeated in two distinct domains, the N- and the C-terminal domains, leading to speculation about a gene duplication and fusion event in its evolution.[2] The N-terminal domain has the closest resemblance to monofunctional peroxidases and contains the single heme group found in each KatG monomer. There are many highly conserved residues, in particular, in the heme cavity where the distal side catalytic histidine and arginine and the proximal side histidine, the iron fifth ligand, are fully conserved among KatGs as well as in monofunctional peroxidases. Situated in the entrance channel leading to the heme cavity are two important residues in KatGs. The first is a serine that is the most frequently identified site of mutation leading to INH resistance in the KatG enzyme of *Mycobacterium tuberculosis* strains. The second is a nearby aspartate that restricts access to the heme cavity.[17] Characteristically, KatGs have a very high proportion of tryptophans, which are used for internal electron transfer and as electron donor sites for protection against oxidation.[18] For example, 23 of 748 residues in *B. pseudomallei* KatG (BpKatG) are tryptophan and of which 15 are in the catalytic N-terminal domain.

Amino acid modifications

Two modifications unique to KatGs were first observed in the crystal structures.[19,20] The first modification, the M-Y-W adduct, was first observed in the crystal structure and then was characterized by mass spectrometry[21] as a cross-linked structure involving the side chains of three fully conserved residues: a methionine, a tyrosine, and a tryptophan. The tyrosine is linked in ortho positions to the methionine and the tryptophan. The second modification, the W-OOH modification, is a perhydroxy group, attached to the indole nitrogen of the adduct tryptophan (see following text).

PROTEIN PRODUCTION, PURIFICATION, AND CHARACTERIZATION

KatG cloning and purification

The first catalase-peroxidase, named hydroperoxidase I or HPI, was isolated from *E. coli* and characterized as a bifunctional, heme-containing protein with a high catalase activity and a broad substrate range peroxidase activity.[22] The gene encoding the enzyme was mapped in 1985 to a locus named *katG*,[23] from which the common name KatG is derived. The gene was subsequently cloned[24,25] and sequenced[16] to provide the first catalase-peroxidase sequence. Most well-characterized KatGs have been overexpressed in an *E. coli* host, in which the KatG gene has been disrupted by a Tn10 transposon. Supplementation of the growth medium with heme generally improves heme occupancy, as determined by the ratio of absorbance at 407 nm (heme) and 280 nm (protein), and the ferric electron paramagnetic resonance (EPR) spectrum, which provides a snapshot of the water

This article was published in the *Encyclopedia of Inorganic and Bioinorganic Chemistry* in 2015 by John Wiley & Sons, Ltd.
DOI: 10.1002/9781119951438.eibc2273

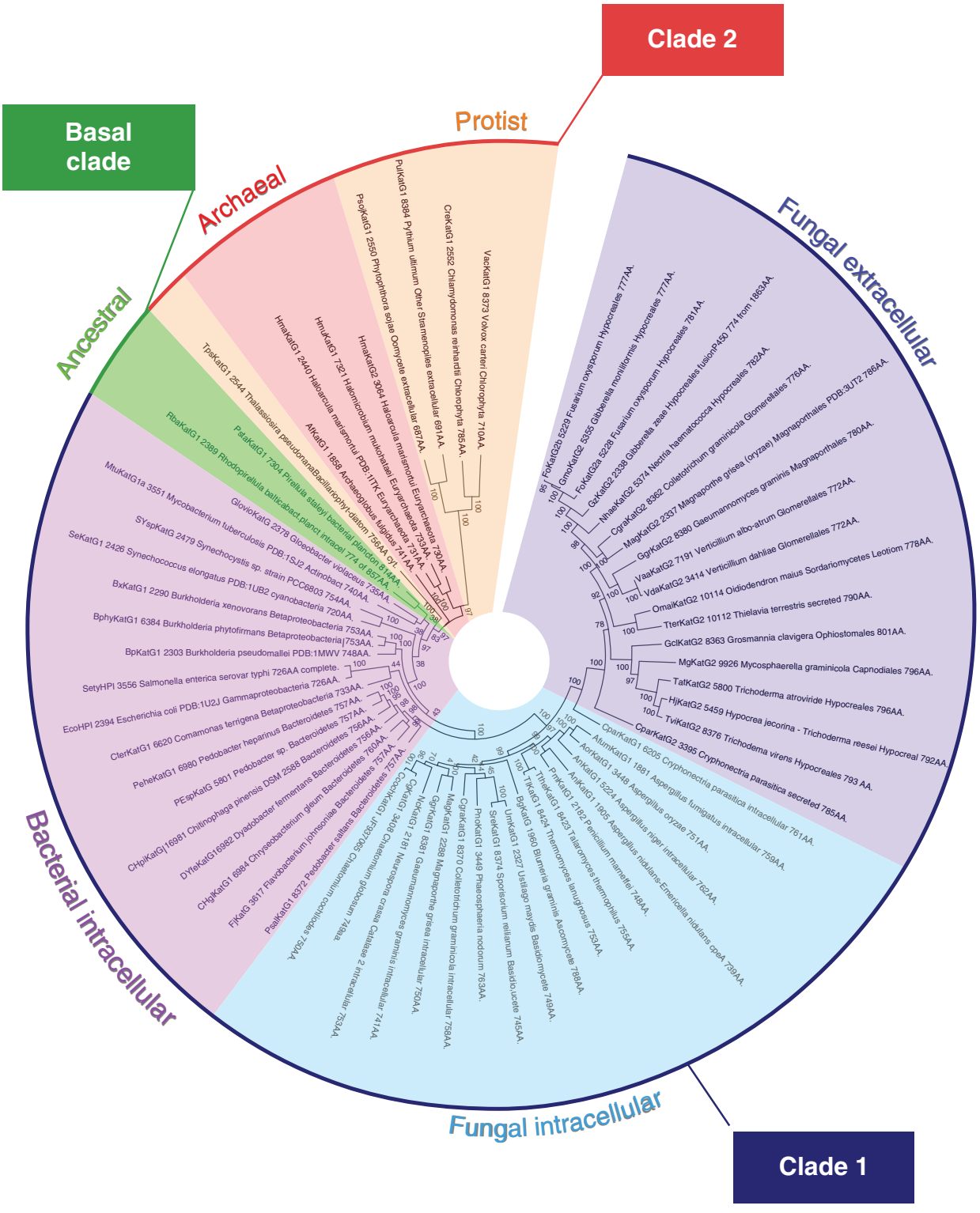

Figure 1 **The catalase-peroxidase family.** Phylogenetic tree showing prokaryotic KatGs and two well-separated clades of eukaryotic catalase-peroxidases, namely a minor clade 2 with protist KatGs and main clade 1 with fungal KatGs consisting of the intracellular KatG1 and extracellular (secreted) KatG2 groups. Abbreviations of sequences and ID numbers correspond with PeroxiBase. Structures deposited in the PDB are also indicated. Molecular phylogeny was reconstructed using the maximum likelihood method of the MEGA 5.05 package[14]. (From Ref. 15. Reproduced by permission of American Society for Biochemistry and Molecular Biology.)

This article was published in the *Encyclopedia of Inorganic and Bioinorganic Chemistry* in 2015 by John Wiley & Sons, Ltd.
DOI: 10.1002/9781119951438.eibc2273

matrix in the cavity. Purification initially involved ion exchange and gel filtration chromatography, but expression with a His-tag has made possible affinity chromatography purification in some cases. The purified enzyme is predominantly a cysteine disulfide cross-linked homodimer of ~160 kDa that can be separated into the component of ~80 kDa monomers by treatment with a sulfhydryl reagent. Bacterial KatGs exhibit reasonable heat resistance with a Tm for inactivation of about 50 °C[26] comparable to the heat resistances of nonsecreted (T_m ~ 45 °C) and secreted (T_m in the 54–60 °C range) eukaryotic KatGs from the phytopathogenic fungus *Magnaporthe grisea*.[15]

Spectroscopy

EPR, resonance Raman, and absorption spectroscopy have been used to characterize the various intermediates that are formed during the reaction cycles.[27,28] The catalatic dismutation of two molecules of hydrogen peroxide to produce two molecules of water and one molecule of oxygen ($2H_2O_2 \rightarrow O_2 + 2H_2O$) occurs in two stages with one molecule of hydrogen peroxide being utilized in each stage, the first as an oxidant and the second as a reductant. In the first stage, the first H_2O_2 oxidizes the heme to a ferryl-oxo species, named compound I (Cpd I or $[Fe^{IV}{=}O\ Por^{\bullet}]^+$), in which one oxidation equivalent is removed from the iron and a second from the porphyrin, with the concomitant production of a water molecule ($[Fe^{III}\ Por]^+ + H_2O_2 \rightarrow [Fe^{IV}{=}O\ Por^{\bullet}]^+ + H_2O$). In the second stage, the second H_2O_2 reduces compound I to regenerate the resting state of the enzyme and a molecule of H_2O along with molecular oxygen, O_2, derived from the two oxygens of the H_2O_2 ($[Fe^{IV}{=}O\ Por^{\bullet}]^+ + H_2O_2 \rightarrow [Fe^{III}\ Por]^+ + H_2O + O_2$). This reaction proceeds through a pathway involving a transient protein radical formed by electron transfer from the M-Y-W adduct to the porphyrin radical of Cpd I ($[Fe^{IV}{=}O\ Por]\ MYW^{\bullet+}$).[29]

The peroxidatic reaction also begins with Cpd I formation, but in the presence of lower H_2O_2 concentrations, electron transfer from specific residues in the protein reduce the porphyrin radical and generate protein radicals ($[Fe^{IV}{=}O\ Por^{\bullet}]^+\ aa \rightarrow [Fe^{IV}{=}O\ Por]\ aa^{\bullet+}$). Trp139, Trp153, and Trp330 in BpKatG[28] have been identified as specific sites of stable radical accumulation in the absence of peroxidatic electron donors. In the presence of an organic peroxidatic substrate (S), the protein radicals and ferryl-oxo species are reduced making the sites of stable radical accumulation actual intermediate steps in electron transfer pathways from the protein surface to the heme ($[Fe^{IV}{=}O\ Por]\ aa^{\bullet+} + 2S + 2H^+ \rightarrow [Fe^{III}\ Por]^+\ aa + 2S^{\bullet+} + H_2O$). A natural peroxidatic substrate of KatGs has not yet been identified, but commonly used laboratory substrates include *o*-dianisidine, pyrogallol, and ABTS (2,2′-azinobis(3-ethylbenzothiazolinesulfonic acid)), which yields a product radical (shown as $2S^{\bullet+}$).

ACTIVITY TESTS

The family of KatGs has remarkably similar kinetic properties regardless of bacterial, archaebacterial, or fungal origin.[15,30] The turnover rates or k_{cat} values for the catalatic reaction all fall in the 3000–8000 s^{-1} range and the K_m values for H_2O_2 are between 2.5 and 4.5 mM at 37 °C. The k_{cat} values for the peroxidatic reaction employing H_2O_2 as oxidant and ABTS as reductant fall in the range 8–25 s^{-1} at 25 °C.[30] Curiously, there is a much broader range of peroxidatic K_m values for H_2O_2 (0.06–1.0 mM) reflecting greater variation in the ease of Cpd I formation as compared to catalatic Cpd I reduction. Similarly, the K_m for ABTS in the peroxidatic process ranges from 7 to 300 μM, most likely a reflection of the differences in ease of electron transfer through the protein from a binding site(s) remote from the heme. The typical catalase reaction monitors the generation of molecular oxygen using an oxygraph equipped with a Clark electrode[31] or following the disappearance of H_2O_2 spectrophotometrically at 240 nm.[32] The advantage of the former technique is that molar concentrations of H_2O_2 can be assayed, thereby precluding the need for extrapolation inherent in the spectrometric assay, which is limited to H_2O_2 concentrations below 5 mM. The peroxidatic reaction is followed by spectrophotometrically monitoring the change in absorbance at a wavelength appropriate for the reaction product (405 nm in the case of ABTS).

The other reactions catalyzed by KatGs all occur at a much slower rate. The INH lyase reaction ($INH + O_2 \rightarrow IN^{\bullet} + HN{=}NH + H^+ + O_2^{\bullet-}$) occurs with a turnover rate of 0.01–0.1 s^{-1}.[30] The NADH oxidase reaction ($NADH + H^+ + O_2 \rightarrow NAD^+ + H_2O_2$ or $NADH + 2O_2 \rightarrow NAD+ + 2\ O_2^{\bullet-}$ depending on pH) occurs at a turnover rate of 0.0001–0.085 s^{-1}.[30] Finally, IN-NAD synthesis ($INH + NAD^+ \rightarrow IN\text{-}NAD + HN{=}NH + H^+$) is catalyzed with a turnover rate of 0.001–0.003 s^{-1}.[30]

X-RAY STRUCTURE

Crystallization

Attempts to crystallize HPI from *E. coli* began in 1987, but have not yet yielded the structure of the complete enzyme, and only the structure of the C-terminal domain has been determined.[33] The first KatG structures reported were from the halophilic archaebacterium *Haloarcula marismortui* (HmKatG) at 2.0 Å resolution[19] and from *B. pseudomallei* (BpKatG) at 1.7 Å[20] (Table 1). Since then, the structures of KatGs have also been determined from two other prokaryotes, *Mycobacterium tuberculosis* (MtKatG)[42,34] and *Synechococcus elongatus* KatG (PDB code 1UB2) – and from one eukaryote, the secreted eukaryotic enzyme from *M. grisea* (MagKatG2).[15] The structures of a large number of variants, in particular, from BpKatG, have also been determined.

This article was published in the *Encyclopedia of Inorganic and Bioinorganic Chemistry* in 2015 by John Wiley & Sons, Ltd.
DOI: 10.1002/9781119951438.eibc2273

Table 1 Catalase-peroxidase structures (April 2014)

PDB ID	Name	Organism	Deposition date	Resolution (Å)	Comment
1ITK[19]	HmKatG	*H. marismortui*	Jan 2002	2.0	Native
1MWV[20]	BpKatG	*B. pseudomallei*	Oct 2002	1.7	Native
1UB2[Unp.]	SeKatG	*S. elongatus*	Mar 2003	2.4	Native
1SJ2[34]	MtKatG	*M. tuberculosis*	Mar 2004	2.4	Native
1U2J[33]	EcKatG	*E. coli*	Jul 2004	2.3	Native ($P2_12_12_1$)
1U2K[33]	EcKatG	*E. coli*	Jul 2004	2.0	Native ($I4_1$)
1U2L[35]	EcKatG	*E. coli*	Jul 2004	2.3	Native (P1)
1X7U[35]	BpKatG	*B. pseudomallei*	Aug 2004	1.9	Mutant S324T
2B2O[36]	BpKatG	*B. pseudomallei*	Sep 2005	1.9	Native, pH 8
2B2Q[36]	BpKatG	*B. pseudomallei*	Sep 2005	2.0	Native, pH 7.5
2B2R[36]	BpKatG	*B. pseudomallei*	Sep 2005	1.9	Cpd I-like
2B2S[36]	BpKatG	*B. pseudomallei*	Sep 2005	2.0	Cpd I-like, pH 7.5
2CCA[37]	MtKatG	*M. tuberculosis*	Jan 2006	2.0	Native
2CCD[37]	MtKatG	*M. tuberculosis*	Jan 2006	2.1	Mutant S315T
2FXG[38]	BpKatG	*B. pseudomallei*	Feb 2006	2.0	Native, pH 4.5
2FXH[38]	BpKatG	*B. pseudomallei*	Feb 2006	1.9	Native, pH 6.5
2FXJ[38]	BpKatG	*B. pseudomallei*	Feb 2006	1.9	Native, pH 8.5
2DV1[39]	BpKatG	*B. pseudomallei*	Jul 2006	1.8	Mutant D141E
2DV2[39]	BpKatG	*B. pseudomallei*	Jul 2006	2.1	Mutant D141E, pH 8
3N3N[5]	BpKatG	*B. pseudomallei*	May 2010	2.1	INH complex
3N3O[5]	BpKatG	*B. pseudomallei*	May 2010	1.7	NAD complex
3N3P[5]	BpKatG	*B. pseudomallei*	May 2010	1.9	INH&AMP complex
3N3Q[5]	BpKatG	*B. pseudomallei*	May 2010	1.9	INH-S324T mutant complex
3N3R[5]	BpKatG	*B. pseudomallei*	May 2010	1.6	Mutant E198A
3N3S[5]	BpKatG	*B. pseudomallei*	May 2010	1.7	INH-E198A mutant complex
3UT2[15]	MgKatG2	*M. grisea*	Nov 2011	1.5	Fungal enzyme
3UW8[Unp.]	HmKatG	*H. marismortui*	Dec 2011	2.3	Mutant S305T
3VLH[Unp.]	HmKatG	*H. marismortui*	Dec 2011	1.7	Mutant R409L
3VLI[Unp.]	HmKatG	*H. marismortui*	Dec 2011	1.7	Cyanide-R409L mutant complex
3VLJ[Unp.]	HmKatG	*H. marismortui*	Dec 2011	1.7	CN-*o*-dianisidine-R409L complex
3VLK[Unp.]	HmKatG	*H. marismortui*	Dec 2011	2.0	Mutant S305A
3VLL[Unp.]	HmKatG	*H. marismortui*	Dec 2011	2.0	Inhibitor-S305A mutant complex
3VLM[Unp.]	HmKatG	*H. marismortui*	Dec 2011	2.3	Mutant M244A
4C50[40]	MtKatG	*M. tuberculosis*	Dec 2011	2.5	Mutant D137S
4C51[40]	MtKatG	*M. tuberculosis*	Dec 2011	3.1	Mutant R418L
4KA5[17]	BpKatG	*B. pseudomallei*	Apr 2013	1.6	Mutant D141A
4KA6[17]	BpKatG	*B. pseudomallei*	Apr 2013	1.7	INH-D141A complex
3WNU[41]	SeKatG	*S. elongatus*	Dec 2013	2.2	Native

For HmKatG, monoclinic crystals, belonging to space group $C2$ ($a = 317.6$ Å, $b = 82.1$ Å, $c = 75.1$ Å, $\beta = 100.2^\circ$), with a reddish brown color and a rhombic plate shape were obtained at 20 °C by the vapor-diffusion, hanging-drop method, with 2 μl of a concentrated protein solution (40–50 mg ml^{-1}) that was not mixed with reservoir solution and was equilibrated against 1.0 ml of 3.0–3.2 M $(NH_4)SO_4$. For BpKatG, orthorhombic crystals, belonging to space group $P2_12_12_1$ ($a = 100.9$ Å, $b = 115.1$ Å, $c = 175.3$ Å), were also obtained at 20 °C and by the vapor-diffusion, hanging-drop method, with 2 μl of a 22 mg ml^{-1} of protein solution and 1 μl of the reservoir solution containing 16–20% (w/v) polyethylene glycol (PEG 4K), 20% (v/v) 2-methyl-2,4-pentanediol (MPD), and 0.1 M sodium citrate, pH 5.6. Both HmKatG and BpKatG crystals contained two subunits, a molecular dimer, in their crystal asymmetric units.

Overall description of the structure

KatGs are normally organized as molecular dimers (as shown in the 3D Structure), although HPI of *E. coli* also forms stable tetramers in solution.[22] The two subunits in the dimer are related by a molecular twofold symmetry and present an extensive contact surface without any significant interdigitation. Each subunit has N- and C-terminal globular domains, both of which are structurally closely related to nonanimal heme peroxidases (Figure 2) consistent with their sequence similarities. The heme pocket

This article was published in the *Encyclopedia of Inorganic and Bioinorganic Chemistry* in 2015 by John Wiley & Sons, Ltd.
DOI: 10.1002/9781119951438.eibc2273

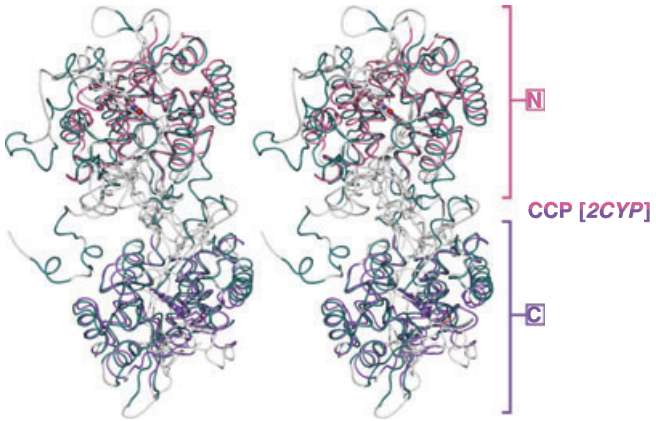

Figure 2 **Peroxidatic fold of the catalase-peroxidase KatG.** Stereo view of the superposition of cytochrome *c* peroxidase (PDB code 2CYP) on both the N-terminal (pink) and the C-terminal (purple) halves of a BpKatG monomer. Loops are light gray and secondary structure elements have been colored accordingly.

Table 2 Heme cavity amino acids and numbering equivalences among KatGs

PDB ID	BpKatG	HmKatG	MgKatG2	MtKatG	SeKatG
Met_{MYW}	M264	M244	M299	M255	M247
Tyr_{MYW}	Y238	Y218	Y273	Y229	Y221
Trp_{MYW}	W111	W95	W140	W107	W93
Arg_{Sw}	R426	R409	R461	R418	R412
His_{Ds}	H112	H96	H141	H108	H94
Arg_{Ds}	R108	R92	R137	R104	R90
Asn_{Ds}	N142	N124	N169	N136	N122
Asp_{Hc}	D141	D125	D170	D137	D123
Ser_{Hc}	S324	S305	S357	S315	S307
His_{Px}	H279	H259	H314	H270	H262
Trp_{Px}	W330	W311	W365	W321	W313
Asp_{Px}	D389	D372	D424	D381	D375

(Figure 3(a)), where a single heme *b* group is found per KatG monomer, is defined exclusively by residues from the N-terminal domain. The C-terminal domain has been subject to greater evolutionary drift compared to other class I peroxidases including loss of the heme-binding pocket, the site of which is occluded by a protein loop.[33]

Heme, heme pocket, and heme channels

KatG monomers contain one heme *b* group that always presents the same orientation as defined by the positions of the methyl and vinyl groups (Figure 3(a) and (b)). A covalent modification, consisting in a most likely perhydroxy modification of the vinyl group of heme ring I, has been reported in one structure of BpKatG.[20,21] In the resting state of KatGs, the heme ferric iron is coordinated with the Nε atom from the proximal histidine as the fifth ligand (Table 2) and with a loosely bound water molecule on the heme distal side (at a distance of ~2.6 Å in BpKatG). This water is often partially displaced, particularly at high pHs, by the perhydroxy modification of the adduct tryptophan (W-OOH) (Figure 3(a)). The heme pocket of KatGs is structurally very closely related to that of class I peroxidases, such as cytochrome *c* peroxidase (CCP) or ascorbate peroxidase (APX), with the catalytically essential residues fully conserved in almost identical arrangements (Figure 3(c)). Thus, the proximal histidine makes a hydrogen bond with a proximal aspartate and shows stacking interactions with a proximal tryptophan (Figure 3(a)). On the distal side, the imidazole moiety of the essential distal histidine is oriented perpendicular to the heme with Nε pointing toward the heme iron at a distance of ~5.5 Å (in BpKatG), whereas Nδ acts as the donor in a hydrogen bond with a conserved distal asparagine. A fully conserved distal arginine is also found in the distal side pocket of both KatGs and class I peroxidases. A most unique feature of KatGs is the presence of the covalent adduct M-Y-W between three residues (Met–Tyr–Trp), with the tryptophan stacked above the heme distal side at just 3.4 Å in the equivalent location to the tryptophan found in the heme distal side of CCP (Figure 3(b)). The angle formed by the adduct tyrosine and tryptophan side chains (~40°) suggests that the bond linking them is not pure sp^2 in character. The methionine of the adduct is most likely carrying a positive charge and this has important implications for the electronic distribution in the adduct. The self-catalytic formation of the covalent adduct has been demonstrated,[43] but it has not been possible to obtain crystals of the protein before the modification is fully formed indicating that the adduct causes a significant structural rearrangement. The adduct is in close association with a fully conserved arginine that can adopt two alternative conformations,

This article was published in the *Encyclopedia of Inorganic and Bioinorganic Chemistry* in 2015 by John Wiley & Sons, Ltd.
DOI: 10.1002/9781119951438.eibc2273

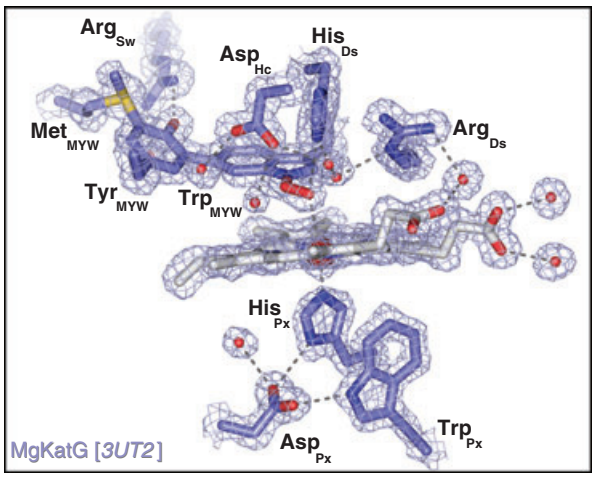

(a)

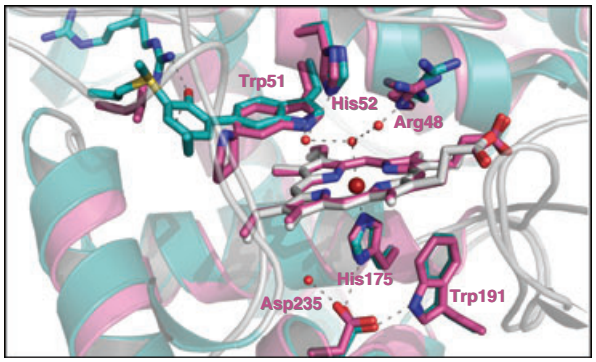

(b)

Figure 3 **Catalase-peroxidase active center.** (a) Close-up view of the heme pocket of MagKatG2 (PDB code 3UT2) showing the presence of the covalent adduct in the proximal side involving the adduct residues methionine (Met_{MYW}), tyrosine (Tyr_{MYW}), tryptophan (Trp_{MYW}), and the swinging arginine (Arg_{Sw}) represented here in the adduct-interacting conformation. In addition, the active-site distal histidine (His_{Ds}), the distal arginine (Arg_{Ds}), the iron coordinating proximal histidine (His_{Px}) – which is in turn H-bonded to the proximal tryptophan (Trp_{Px}) – and the proximal aspartate (Asp_{Px}) are also depicted. The Trp_{MYW} appears peroxidized on the indole nitrogen. (b) Active center view of a superposed cytochrome *c* peroxidase (Figure 1(b)) on the N-terminal half of BpKatG. Except for Met_{MYW} and Tyr_{MYW} (whose structural equivalents would be a Lys and a Pro, respectively), the remaining distal Trp_{MYW}, His_{Ds}, and Arg_{Ds} together with the proximal His_{Px}, Trp_{Px}, and Asp_{Px} are conserved residues in cytochrome *c* peroxidase (corresponding to Trp51, His52, and Arg48 – on the distal side – and His175, Trp191, and Asp235 – on the proximal side).

one of which establishes an ionic interaction with the adduct tyrosine when its hydroxyl group is deprotonated (Figure 4). Adduct residues and this swinging arginine have been shown to be essential for the catalatic reaction but not for the peroxidatic one.[44]

The most obvious access route to the distal side of the heme is provided by a heme access channel positioned similarly to (Figure 5, in orange), but longer and more constricted than, the access route in peroxidases. This channel has a pronounced funnel shape and is narrowest just before entering the heme pocket, where two conserved important residues – a serine and an aspartate – are found (see following text), with a continuum of water molecules clearly defined in many of the structures determined.[20] In addition, the distal side arginine, working in concert with a distal aspartate in the main heme entry channel also influence access to the heme cavity.[44,39] Most peroxidases have a second access route, approximately in the plane of the heme, leading to the distal side. However, in KatGs, this second route appears to be blocked by the extended loops suggesting that substrates entering and products released from the heme pocket all use the funnel-shaped channel. However, there does appear to be at least one other entrance to reach the core of a subunit starting at the molecular twofold axis and approaching the swinging arginine (Figure 5, in purple). While a functional role for this 'back door' entrance to KatGs has not been demonstrated, it has been shown to be the binding side of chlorine and also of the antitubercular drug INH in BpKatG.[5]

N-terminal extension

KatGs have an extension at their N-terminal end of about 60 residues compared to nonanimal peroxidases. Approximately half of this extension is disordered or not visible in all the structures determined, likely indicating a considerable degree of flexibility despite the presence of a cysteine (Cys27 in BpKatG) that may form a disulfide bridge between the two subunits of the dimer.[45] This cysteine is highly conserved in nonarchaeal KatGs as part of a CP motif (Figure 6(a)). These CP regions have been shown to act as heme-binding motifs[46] and to show heme recruitment, heme sensing, and regulatory effects,[46–49] although none of these capabilities has yet been identified in KatGs. In fact, replacement of this residue by a Ser altered neither enzyme dimerization nor its enzymatic activity.[50]

Secreted eukaryotic KatGs have an even longer N-terminus – around 20 residues – when compared to both bacterial and nonsecreted eukaryotic KatGs (Figure 6(a)), which includes the CP motif and two extra cysteines that form two dimeric intersubunit disulfide bridges (Figure 6(b)). Part of this extended N-terminus, visible in the structure of the only eukaryotic KatG structure available[15] (3UT2), is filling the cleft between the two subunits, increasing the dimerization surface.

In addition to subunit intertwining, a likely physiological role is suspected as the intersubunit disulfide bridges are conserved in all secreted KatGs. In fact, cysteine mutations in MgKatG results in a melting temperature decrease

This article was published in the *Encyclopedia of Inorganic and Bioinorganic Chemistry* in 2015 by John Wiley & Sons, Ltd.
DOI: 10.1002/9781119951438.eibc2273

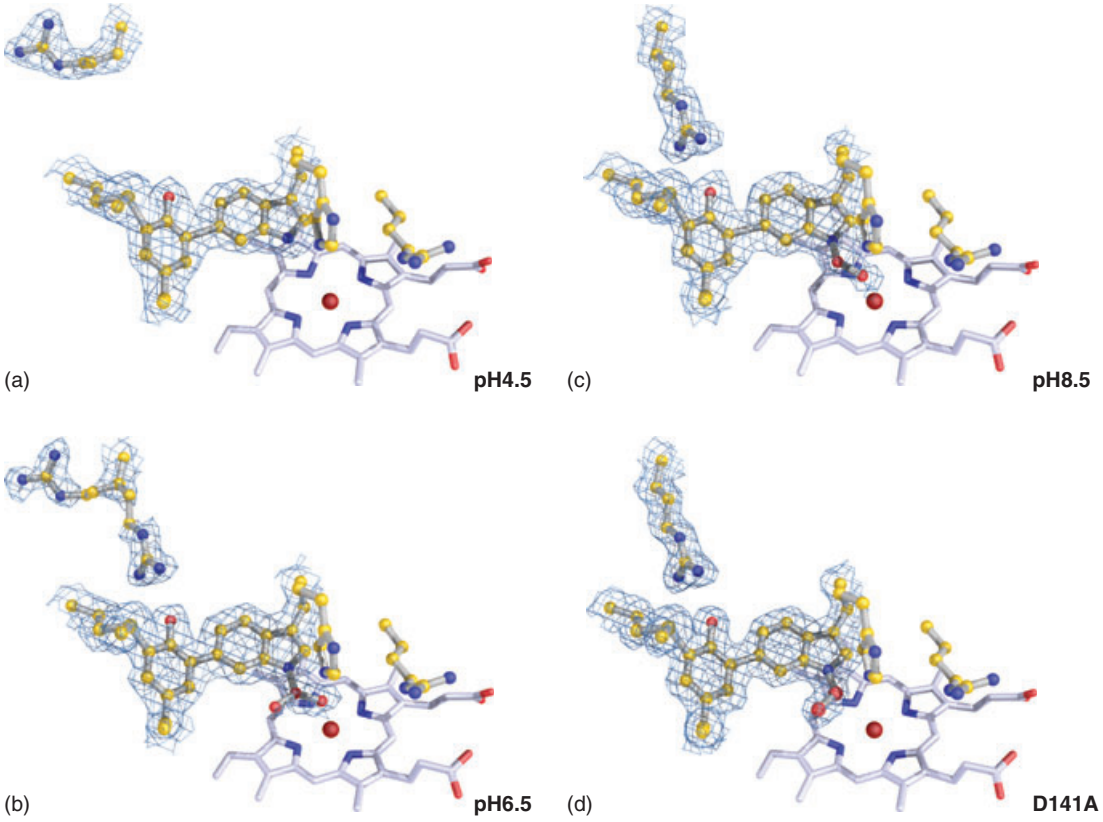

Figure 4 **Interaction of the M-Y-W adduct with the swinging Arg_{Sw}.** Crystal structures of BpKatG showing changes in the peroxidation of the Trp_{MYW} and in the relative disposition of the two conformations of Arg_{Sw}. (a) PDB code: 2FXG, native BpKatG at pH 4.5, (b) PDB code: 2FXH, native BpKatG at pH 6.5, (c) PDB code: 2FXH, native BpKatG at pH 8.5, and (d) PDB code: 4KA5, mutant D141A of BpKatG.

showing that the disulfide bridges are essential for protein stability.[15]

COMPLEX STRUCTURES

If a crystal of BpKatG is soaked briefly with a peracetate solution, the heme iron will turn to a ferryl-oxo species by addition of an oxygen atom similar to what has been observed in both monofunctional catalases and peroxidases.[36] However, in the ferryl-oxo BpKatG complex at 1.9 Å resolution,[36] the iron to oxygen distance was ~2.0 Å (Figure 7(a)), longer than expected for a classic Cpd I species (~1.6 Å) containing a porphyrin cation radical. The longer Fe–O bond length is explained by facile electron transfer within the protein reducing the porphyrin radical to a Cpd I* species {aa$^{\bullet\ddagger}$ [Por Fe^{IV}–OH]$^{+}$} with a longer iron to oxygen bond length of 1.8–2.0 Å (Figure 7(b)). The only other significant change in the structure of the ferryl-oxo BpKatG species with respect to the resting enzyme was a shift in the position of the swinging arginine adopting a single conformation away from the interaction with the adduct tyrosine. Changes in conformation of the swinging arginine have been rationalized in terms of modulating the transfer of electrons between the heme group and the adduct that are essential for the catalase reaction.[36]

The activation of INH by BpKatG and MtKatG involves removal of the diimide and one electron from INH to create an isonicotinyl radical (IN$^{\bullet}$), which then reacts with NAD^{+}. The resulting isonicotinyl-NAD radical (IN-$NAD^{+\bullet}$) is then reduced by superoxide ($O_2^{-\bullet}$) to isonicotinyl-NAD, the active form of the drug that inhibits mycolic acid synthesis.[5] The principal roles played by KatGs in this process appear to lie in the enhancement of the rate of INH breakdown to the isonicotinyl radical and the generation of superoxide. Subsequent reaction of the isonicotinyl radical with NAD^{+} and reduction of the isonicotinyl-NAD radical by superoxide ion are only marginally influenced by KatG except possibly by enhanced superoxide production. The binding sites, found in complexes of BpKatG with INH and NAD^{+} (Figure 8(a) and (b)), can be interpreted as being consistent with this mechanism.[5] INH was found at the opening of the potential back

This article was published in the *Encyclopedia of Inorganic and Bioinorganic Chemistry* in 2015 by John Wiley & Sons, Ltd.
DOI: 10.1002/9781119951438.eibc2273

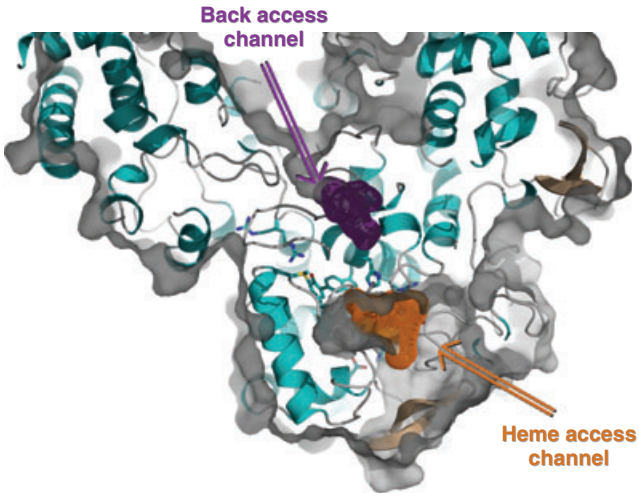

Figure 5 **Molecular channels in catalase-peroxidases.** Molecular surface (in gray) of a BpKatG subunit showing two channels that lead to the heme pocket: the main heme access channel (in orange) and a 'back door entrance' secondary channel (in purple) that appears interrupted close to the adduct region. From the corresponding cavities (calculated with program Hollow, http://hollow.sourceforge.net), the final part has been depicted by dense dots.

door entrance (see previous section) about 10 Å from a site of stable radical accumulation in BpKatG (Trp139). While the corresponding radical sites have not been confirmed in MtKatG, INH has been shown to reduce similar protein radicals in that enzyme.[28] A BpKatG-NAD^+ complex was also crystallized leading to the identification of a NAD^+ binding site on the surface of the protein about 20 Å from the main entrance channel to the heme. This binding site was intriguing mainly for two reasons. The first was its significant separation from the INH binding site, which suggested that one or both of the isonicotinyl radical and NAD^+ had to dissociate from their binding sites to find the other reactant. The second was that the binding site, evident only in one subunit at the surface of the protein, suggested a weak binding easily affected by crystal packing and crystallization conditions. Thus, despite NADH being a known substrate for KatG in a location where NAD^+ acts as a competitive inhibitor, the binding site for the nucleotide remains uncertain.

Recently, the complex of a BpKatG variant of the aspartate at the entrance of the heme channel (D141A) with INH has been obtained (Figure 8(c)), showing the presence of INH inside the heme distal pocket. This residue is fully conserved in KatGs but is absent in other nonanimal peroxidases. This residue is situated at the heme pocket entrance in the narrowest location of the heme entrance funnel.

FUNCTIONAL ASPECTS

Modeling studies and the catalatic reaction mechanism in KatGs

Quantum mechanics and dynamics simulations have provided invaluable insights into the reaction mechanisms of catalase-peroxidase KatGs and the possible roles of the adduct and the swinging arginine in the catalatic process.[51,52] Density functional theory (DFT) calculations using quantum mechanics/molecular mechanics (QM/MM) models of an oxyferryl Cpd I species, including in the quantic description, the close heme environment and the M-Y-W adduct, suggest that spin density localizes on the adduct only when the adduct tyrosine is unprotonated and not associated to the swinging arginine. Protonation of the adduct tyrosine or association with the swinging arginine leads to spin density accumulation on the proximal tryptophan similar to what is expected to happen in peroxidase CCP.[51] Significantly, little spin density was found on the heme suggesting a relatively unstable heme radical consistent with its rapid reduction and formation of stable protein radicals in residues away from the heme such as Trp139 and Trp153 in BpKatG. These calculations were therefore suggestive of a transient protein radical being formed on the adduct. Experimental evidence has been gathered either by the direct determination of such transient radical[29] or indirectly, implicating the adduct radical in the reaction of KatGs with molecular oxygen to form the perhydroxy modification on the adduct tryptophan indole and superoxide in the presence of electron donors such as INH.[52]

Recently, a model of the catalatic reaction in KatGs has been proposed[53] (Figure 9), which integrates most of the experimental observations and computational calculations obtained to date. According to this model, the interplay of the adduct M-Y-W with the swinging arginine makes possible the catalatic activity in catalase-peroxidases. Once the active Cpd I is formed, the arginine, acting as a pH-dependent electronic switch, controls the localization of a radical in the adduct and in doing so, does also modify the adduct tryptophan reactivity enabling its indole to deprotonate. The consequent indole proton transfer is capable to promote the reduction of Cpd I with a second H_2O_2 molecule in much the same way as the acid/base distal histidine in catalase does.

ACKNOWLEDGMENTS

This work was supported by the Spanish Ministerio de Ciencia e Innovación grant BFU2012-36827 (to I.F.), Discovery Grant 9600 from the Natural Sciences and Engineering Research Council of Canada (to P.C.L.), the Canada Research Chair Program (to

This article was published in the *Encyclopedia of Inorganic and Bioinorganic Chemistry* in 2015 by John Wiley & Sons, Ltd.
DOI: 10.1002/9781119951438.eibc2273

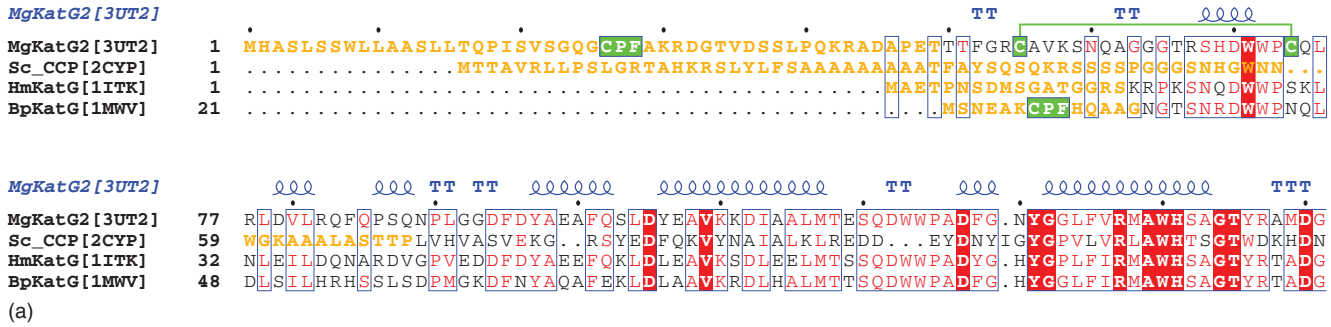

(a)

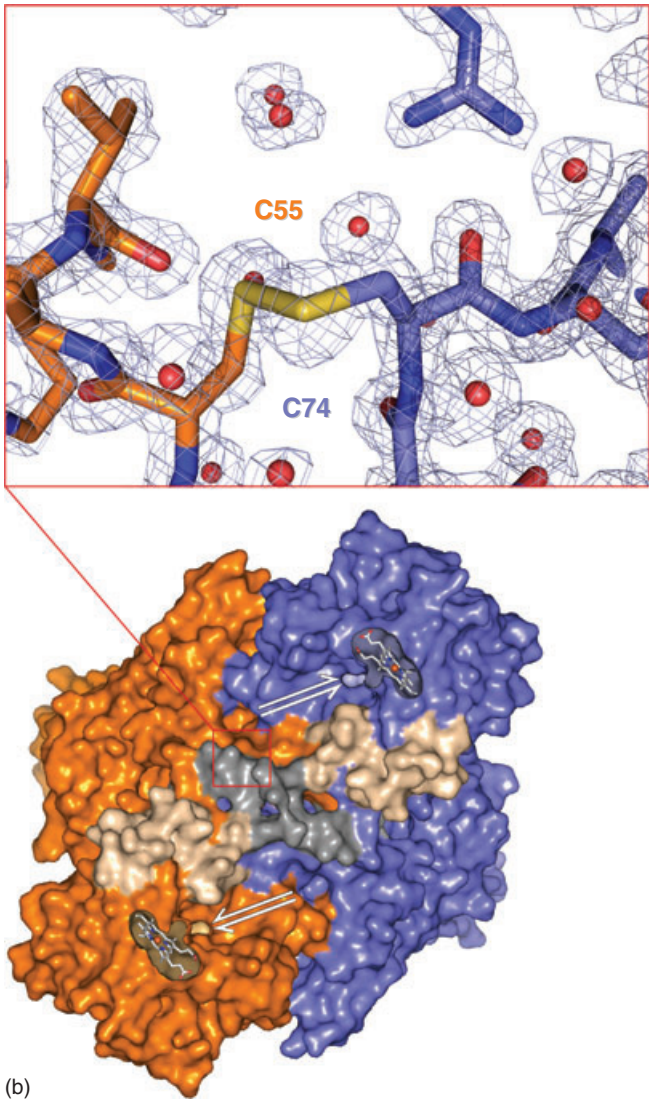

(b)

Figure 6 **The N-terminal region of catalase-peroxidases.** (a) Structural alignment of the N-terminal region of representative KatGs (archeobacterial 1ITK, bacterial 1MWV, and fungal 3UT2) and cytochrome *c* peroxidase (2CYP). The secondary structural motifs of the longest N-terminus from MagKatG2 structure are included in the alignment. Residues not seen in the corresponding structures are depicted in yellow. Except for archeobacterial KatGs – which are devoid of cysteines – the CPF motif is present in all KatG sequences. In addition, two extra Cys residues that form two intersubunit disulfide bonds in secreted KatGs are present. (b) The disulfide bridge clearly identified in the 1.55 Å crystal structure of MagKatG2[15] (depicted as dark gray on the dimer surface representation). The extended (compared to other KatGs) N-terminus of secreted KatG increase the dimerization surface (in beige) by filling up the space between both monomers on the surface that leads to the heme access channel (signaled with white arrows). (From Ref. 15. Reproduced by permission of American Society for Biochemistry and Molecular Biology.)

This article was published in the *Encyclopedia of Inorganic and Bioinorganic Chemistry* in 2015 by John Wiley & Sons, Ltd.
DOI: 10.1002/9781119951438.eibc2273

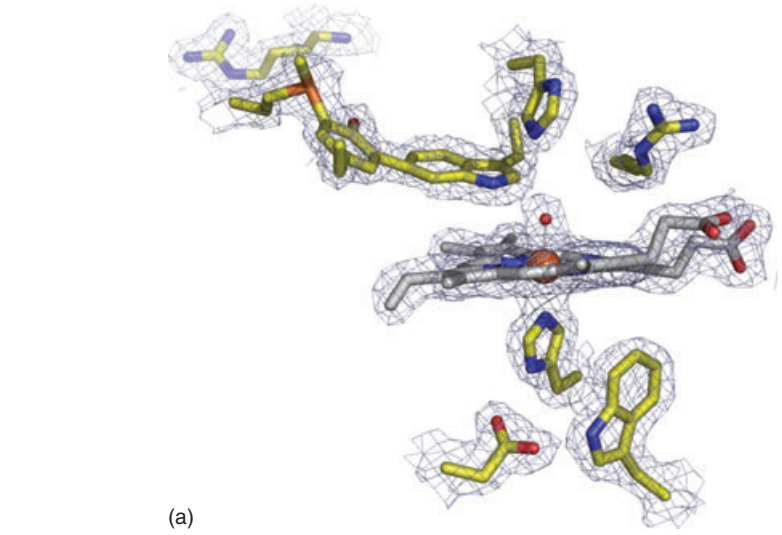

(a)

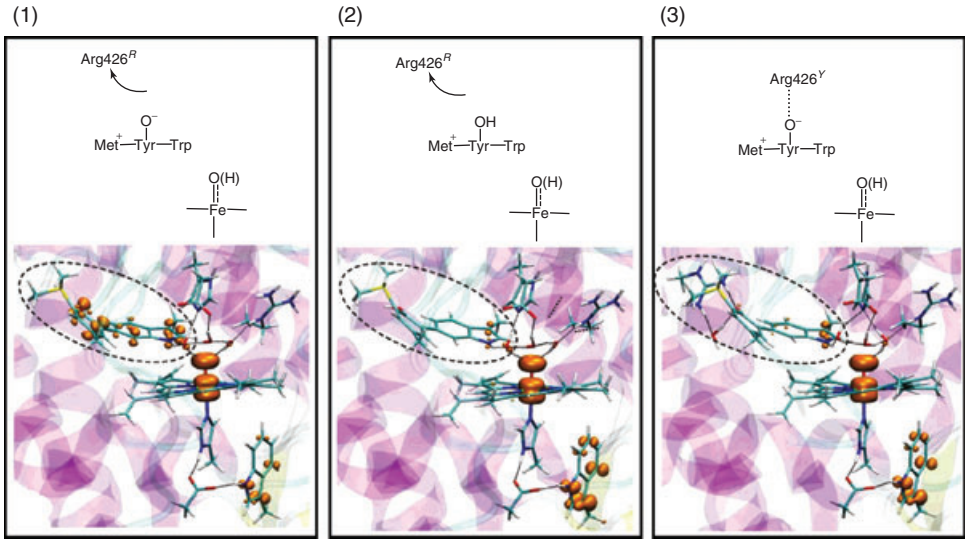

(b)

Iron–Oxygen distance (Å) in Cpds I and II

	Fe=O	Fe–OH
Ia	1.71	1.85
Ib	1.71	1.82

Figure 7 **Oxoferryl complex.** (a) View of the active center complex of BpKatG obtained after soaking with peroxoacetic acid[36] (PDB code: 2B2S). The swinging Arg_{Sw} acts as an electronic switch, allowing to store a protein radical – at least transiently – in the adduct. (b) Considering three different possibilities (1, 2, and 3) for the Arg_{Sw} ↔ adduct interaction, by means of QM/MM calculations, it has been shown that the electronic spin density is distributed among the adduct residues or the proximal Trp after H_2O_2 oxidation of the enzyme to Cpd I intermediate. The experimentally observed iron–oxygen distance in this oxoferryl complex (1.88 Å) is longer than the calculated one for Cpd I (see adjunct table). Showing it is an oxoferryl species in a midpoint between Cpd I and Cpd II intermediates. (B.1) The Arg_{Sw} in the R conformation, while the adduct Tyr_{MYW} is deprotonated, whereas in (B.2), it is protonated. Finally, in (B.3), the Arg_{Sw} is directly interacting with the adduct through a salt bridge with the deprotonated Tyr_{MYW}. (Reprinted with permission from Ref. 51. Copyright (2007) American Chemical Society.)

This article was published in the *Encyclopedia of Inorganic and Bioinorganic Chemistry* in 2015 by John Wiley & Sons, Ltd.
DOI: 10.1002/9781119951438.eibc2273

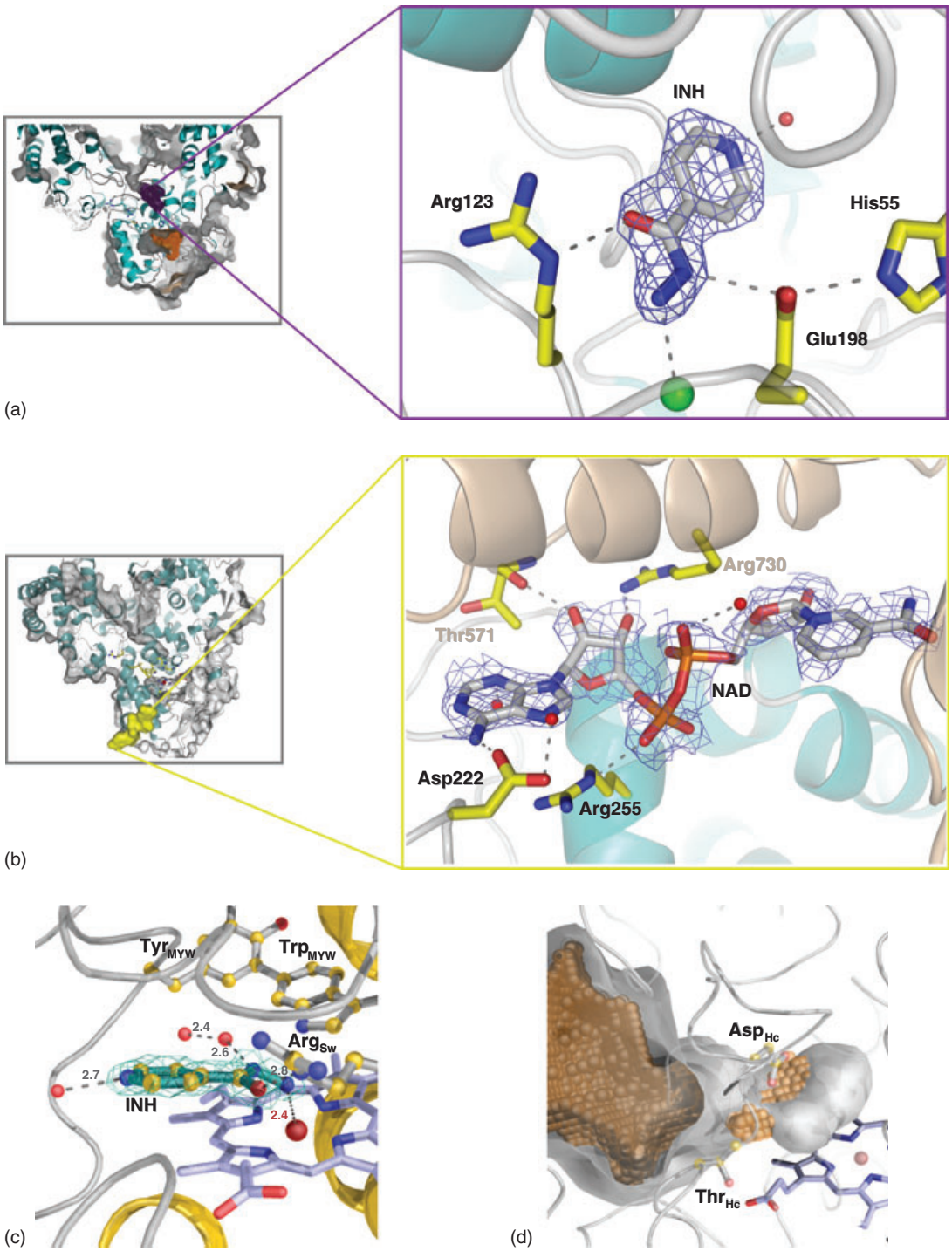

Figure 8 **INH and NAD complexes.** (a) INH molecule located in the back access channel of BpKatG[5] (PDB code: 3N3N). (b) An NAD molecule (with a disordered nicotinamide region) was located between symmetry-related subunits (depicted in cyan and beige, respectively), far away from the INH site (PDB code: 3N3O). (c) An INH molecule was located inside the heme cavity in D141A mutant of BpKatG (PDB code: 4KA6) as previously predicted by QM/MM calculations.[17] (d) Two residues line up the heme access channel where there is a constriction: Ser_{Hc} (whose S315T mutation has been found responsible of the main INH resistance in strains of *M. tuberculosis*) and Asp_{Hc}. Mutating the latter to Ala allows a widening of the channel and permits the INH molecule to reach the heme vicinity as it occurred in D141A mutant of BpKatG.[17]

This article was published in the *Encyclopedia of Inorganic and Bioinorganic Chemistry* in 2015 by John Wiley & Sons, Ltd.
DOI: 10.1002/9781119951438.eibc2273

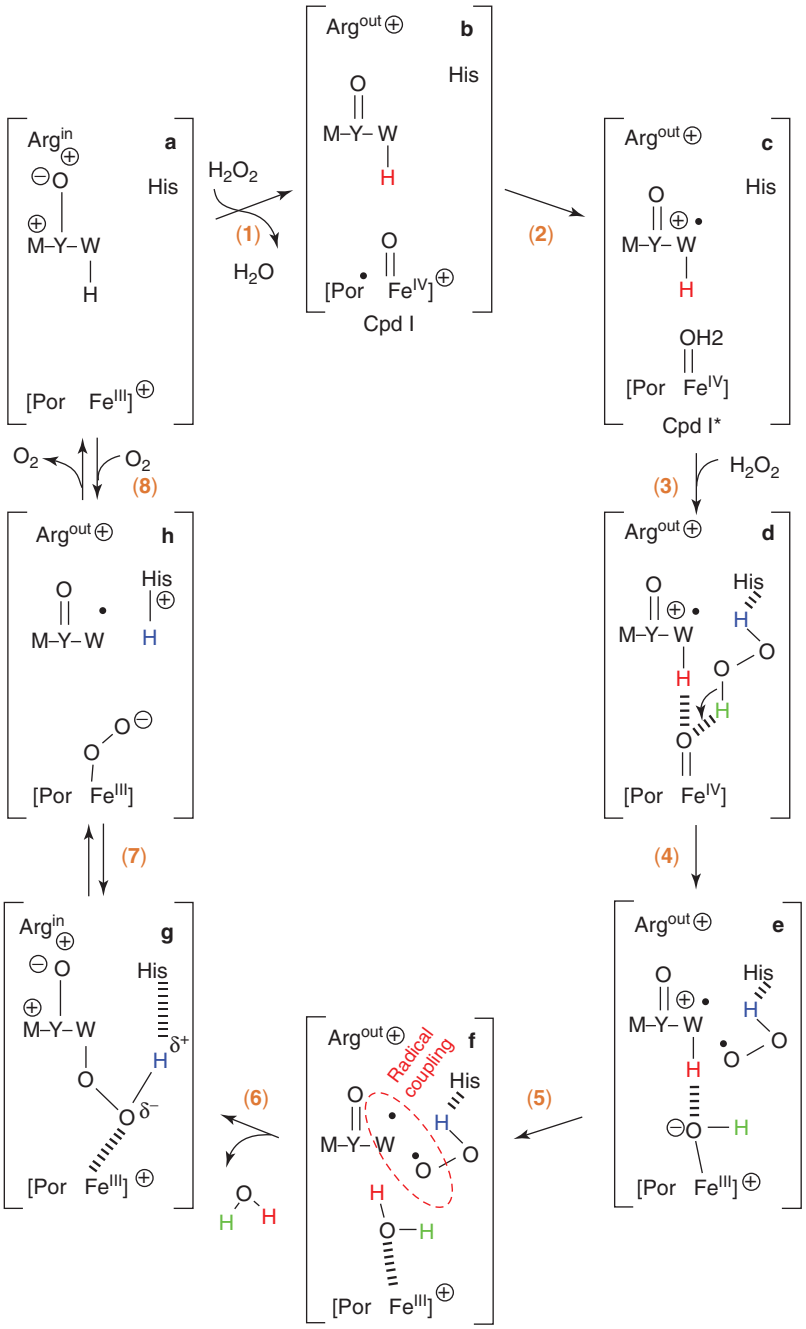

Figure 9 **Catalatic reaction pathway in KatGs.** The recently proposed mechanism[53] includes the following steps: (1) Cpd I formation after reaction of the native enzyme with an H_2O_2 molecule; (2) the oxidation equivalent on the porphyrin migrates and accumulates on the M-Y-W adduct, producing a Cpd I* intermediate in a pH range where the catalatic activity is optimal (pH ~7); (3) a second H_2O_2 molecule binds to the active center; (4) an H_2O_2 hydrogen atom is transferred to Cpd I*, producing an $HO_2^{\bullet}$ radical and a ferric Fe^{III}–OH; (5) the adduct tryptophan, in a similar orientation as the catalytic distal histidine in catalases, transfers a proton to the hydroxoferryl oxygen with a concomitant water molecule formation; (6) radical coupling of $MYW^{\bullet+}$ and $HO_2^{\bullet}$; (7) the breakage of the N (Trp)-OOH bond leads to the formation of a ferric superoxo species (Fe^{III}–$O_2^{\bullet-}$) and an adduct radical; and (8) finally, upon loss of O_2 from Fe^{III}–$O_2^{\bullet-}$ and an electron transfer to the adduct, the resting state is recovered. All species (**a**–**h**) have been characterized either by X-ray crystallography or by QM/MM calculations.

This article was published in the *Encyclopedia of Inorganic and Bioinorganic Chemistry* in 2015 by John Wiley & Sons, Ltd.
DOI: 10.1002/9781119951438.eibc2273

P.C.L.), and Generalitat de Catalunya BP-B2008-00239 (to X.C.). Special acknowledgment is given to Pietro Vidossich, Carme Rovira, Marcel Zamocky, and Christian Obinger, for the very fruitful collaborations established around KatGs throughout all those years.

REFERENCES

1 The PyMOL Molecular Graphics System, Version 1.5.0.3 Schrödinger, LLC.

2 KG Welinder, JM Mauro, and L Nørskov-Lauritsen, *Biochem Soc Trans* (1992), **20**, 337.

3 M Zámocký, B Gasselhuber, PG Furtmüller, and C Obinger, *Arch Biochem Biophys*, **525**, 131 (2012).

4 OJ Njuma, EN Ndontsa, and DC Goodwin, *Arch Biochem Biophys*, **544C**, 27 (2014).

5 B Wiseman, X Carpena, M Feliz, LJ Donald, M Pons, I Fita, and PC Loewen, *J Biol Chem*, **285**, 26662 (2010).

6 MG Klotz and PC Loewen, *Mol Biol Evol*, **20**, 1098 (2003).

7 P Chelikani, I Fita, and PC Loewen, *Cell Mol Life Sci*, **61**, 192 (2004).

8 M Zamocky, PG Furtmüller, M Bellei, G Battistuzzi, J Stadlmann, J Vlasits, and C Obinger, *Biochem J*, **418**, 443 (2009).

9 PC Loewen, J Switala, and BL Triggs-Raine, *Arch Biochem Biophys*, **243**, 144 (1985).

10 G Storz, LA Tartaglia, and BN Ames, *Science*, **248**, 189 (1990).

11 SG Rhee, SW Kang, W Jeong, T.-S Chang, K.-S Yang, and HA Woo, *Curr Opin Cell Biol*, **17**, 183 (2005).

12 SE Schriner, NJ Linford, GM Martin, P Treuting, CE Ogburn, M Emond, PE Coskun, W Ladiges, N Wolf, H Van Remmen, DC Wallace, and PS Rabinovitch, *Science*, **308**, 1909 (2005).

13 SG Rhee, *Science*, **312**, 1882 (2006).

14 K Tamura, G Stecher, D Peterson, A Filipski, and S Kumar, *Mol Biol Evol*, **30**, 2725 (2013).

15 M Zámocký, Q García-Fernández, B Gasselhuber, C Jakopitsch, PG Furtmüller, PC Loewen, I Fita, C Obinger, and X Carpena, *J Biol Chem*, **287**, 32254 (2012).

16 BL Triggs-Raine, BW Doble, MR Mulvey, PA Sorby, and PC Loewen, *J Bacteriol*, **170**, 4415 (1988).

17 P Vidossich, PC Loewen, X Carpena, G Fiorin, I Fita, and C Rovira, *J Phys Chem B*, **118**, 2924 (2014).

18 A Ivancich, LJ Donald, J Villanueva, B Wiseman, I Fita, and PC Loewen, *Biochemistry*, **52**, 7271 (2013).

19 Y Yamada, T Fujiwara, T Sato, N Igarashi, and N Tanaka, *Nat Struct Biol*, **9**, 691 (2002).

20 X Carpena, S Loprasert, S Mongkolsuk, J Switala, PC Loewen, and I Fita, *J Mol Biol*, **327**, 475 (2003).

21 LJ Donald, OV Krokhin, HW Duckworth, B Wiseman, T Deemagarn, R Singh, J Switala, X Carpena, I Fita, and PC Loewen, *J Biol Chem*, **278**, 35687 (2003).

22 A Claiborne and I Fridovich, *J Biol Chem*, **254**, 4245 (1979).

23 PC Loewen, BL Triggs, CS George, and BE Hrabarchuk, *J Bacteriol*, **162**, 661 (1985).

24 PC Loewen, BL Triggs, GR Klassen, and JH Weiner, *Can J Biochem Cell Biol*, **61**, 1315 (1983).

25 BL Triggs-Raine and PC Loewen, *Gene*, **52**, 121 (1987).

26 J Switala, JO O'Neil, and PC Loewen, *Biochemistry*, **38**, 3895 (1999).

27 A Ivancich, C Jakopitsch, M Auer, S Un, and C Obinger, *J Am Chem Soc*, **125**, 14093 (2003).

28 R Singh, J Switala, PC Loewen, and A Ivancich, *J Am Chem Soc*, **129**, 15954 (2007).

29 J Suarez, K Ranguelova, AA Jarzecki, J Manzerova, V Krymov, X Zhao, S Yu, L Metlitsky, GJ Gerfen, and RS Magliozzo, *J Biol Chem*, **284**, 7017 (2009).

30 R Singh, B Wiseman, T Deemagarn, V Jha, J Switala, and PC Loewen, *Arch Biochem Biophys*, **471**, 207 (2008).

31 M Rorth and PK Jensen, *Biochim Biophys Acta*, **139**, 171 (1967).

32 H Aebi, *Methods Enzymol*, **105**, 121 (1984).

33 X Carpena, W Melik-Adamyan, PC Loewen, and I Fita, *Acta Crystallogr D Biol Crystallogr*, **60**, 1824 (2004).

34 T Bertrand, N. A. J Eady, JN Jones, J. J. M Nagy, B Jamart-Grégoire, EL Raven, and KA Brown, *J Biol Chem*, **279**, 38991 (2004).

35 T Deemagarn, X Carpena, R Singh, B Wiseman, I Fita, and PC Loewen, *J Mol Biol*, **345**, 21 (2005).

36 X Carpena, B Wiseman, T Deemagarn, R Singh, J Switala, A Ivancich, I Fita, and PC Loewen, *EMBO Rep*, **6**, 1156 (2005).

37 X Zhao, H Yu, S Yu, F Wang, JC Sacchettini, and RS Magliozzo, *Biochemistry*, **45**, 4131 (2006).

38 X Carpena, B Wiseman, T Deemagarn, B Herguedas, A Ivancich, R Singh, PC Loewen, and I Fita, *Biochemistry*, **45**, 5171 (2006).

39 T Deemagarn, B Wiseman, X Carpena, A Ivancich, I Fita, and PC Loewen, *Proteins*, **66**, 219 (2007).

40 X Zhao, H.-P Hersleth, J Zhu, KK Andersson, and RS Magliozzo, *Chem Commun (Camb)*, **49**, 11650 (2013).

41 S Kamachi, K Wada, M Tamoi, S Shigeoka, and T Tada, *Acta Crystallogr F Struct Biol Commun*, **70**, 288 (2014).

42 Y Zhang, B Heym, B Allen, D Young, and S Cole, *Nature*, **358**, 591 (1992).

43 RA Ghiladi, GM Knudsen, KF Medzihradszky, and P. R. Ode Montellano, *J Biol Chem*, **280**, 22651 (2005).

44 G Smulevich, C Jakopitsch, E Droghetti, and C Obinger, *J Inorg Biochem*, **100**, 568 (2006).

45 M Wilming and K Johnsson, *FEBS Lett*, **509**, 272 (2001).

46 L Zhang and L Guarente, *EMBO J*, **14**, 313 (1995).

47 JT Lathrop and MP Timko, *Science*, **259**, 522 (1993).

48 X Yao, P Balamurugan, A Arvey, C Leslie, and L Zhang, *Biochem Biophys Res Commun*, **403**, 30 (2010).

49 T Shimizu, *J Inorg Biochem*, **108**, 171 (2012).

50 B Saint-Joanis, H Souchon, M Wilming, K Johnsson, PM Alzari, and ST Cole, *Biochem J*, **338**(Pt 3), 753 (1999).

51 P Vidossich, M Alfonso-Prieto, X Carpena, PC Loewen, I Fita, and C Rovira, *J Am Chem Soc*, **129**, 13436 (2007).

52 P Vidossich, X Carpena, PC Loewen, I Fita, and C Rovira, *J Phys Chem Lett*, **2**, 196 (2011).

53 PC Loewen, X Carpena, P Vidossich, I Fita, and C Rovira, *J Am Chem Soc*, **136**, 7249 (2014). DOI: 10.1021/ja502794e.

This article was published in the *Encyclopedia of Inorganic and Bioinorganic Chemistry* in 2015 by John Wiley & Sons, Ltd.
DOI: 10.1002/9781119951438.eibc2273